Available online at www.sciencedirect.com
ScienceDirect
Planetary and Space Science 56 (2008) 947–950
Planetary and Space Science
www.elsevier.com/locate/pss

Estimation of solar illumination on the Moon: A theoretical model

Xiongyao Li[a], Shijie Wang[a,*], Yongchun Zheng[c], Anyun Cheng[a,b]

[a]The State Key Laboratory of Environmental Geochemistry, Institute of Geochemistry, Chinese Academy of Sciences, Guiyang 550002, China
[b]Graduate University of the Chinese Academy of Sciences, Beijing 100049, China
[c]The National Astronomical Observatories, Chinese Academy of Sciences, Beijing 10012, China

Received 21 November 2007; received in revised form 15 February 2008; accepted 18 February 2008
Available online 26 February 2008

Abstract

The solar illumination conditions on the lunar surface represent a key resource with respect to returning to the Moon. As a supplement to mapping the solar illumination by exploring data, lighting simulations using high-resolution topography could produce quantitative illumination maps. In this study, a theoretical model is proposed for estimating the solar illumination conditions. It depends only on the solar altitude and topographical factors. Besides the selenographic longitude and latitude, the former is determined by the selenographic longitude and latitude at the subsolar site, the geocentric ecliptical latitude, and the dimensionless distance of the Sun–Moon relative to 1 AU, which are function of time. The latter is determined by comparing the elevations in solar irradiance direction within 210 km in which the topography might shadow the behind sites to the critical elevations determining whether the behind sites are shadowed or not. Compared to Zuber's model, the model proposed in this study is simpler and easier for computing. It is parameterized with selenographic coordinates, elevations, and time. With high-resolution topography data, the solar illumination conditions at any selenographic coordination could be estimated by this model at any date and time. The lunar surface is illuminated when the solar altitude is non-zero and all the elevations within 210 km in solar irradiance direction are lower than the critical elevations. Otherwise it would be shadowed.

Keywords: Moon; Illumination; Model

1. Introduction

The solar illumination conditions represent a key resource with respect to returning to the Moon. Because the Moon's spin axis is nearly perpendicular to the ecliptic plane, it results in different lighting conditions at the lunar poles. Areas which have low elevation, such as the floors of impact craters, may never be directly illuminated by the Sun, i.e. they are permanently shadowed, whilst regions of high elevation, relative to the local terrain, may be permanently illuminated (Bussey and Spudis, 2004). The presence of hydrogen has been detected near the lunar poles (Feldman et al., 1998, 2000). The areas with enhanced hydrogen content are generally coincident with areas permanently in shadow (Margot et al., 1999; Feldman et al., 2001). The temperature in the permanently shaded regions is low enough to trap water ice and other volatiles over the age of the solar system (Vasavada et al., 1999), and the lunar rotation axis has been stable for at least 2 billion years. If the hydrogen is in the form of water ice, it would confirm the idea postulated by Watson et al. (1961) and debated by many scientists since (Arnold, 1979; Butler, 1997; Starukhina, 2001; Hodges, 2002) that ice might exist in lunar cold traps. Beside water ice, other volatiles might also be enriched in permanent shadow at the lunar poles. Reservoirs of volatiles in permanent shadows are scientifically valuable and maybe a potential in situ resource for future exploration.

The solar illumination condition is also an important parameter for site selection, when considering a landing on the lunar surface and building a lunar base. It impacts heavily the landing of the lunar rover and the human activities on the Moon. It should be considered in mission timing, duration and return, as well as design of subsystem (Kruijff and Ockels, 1995).

For these reasons, analysis of the lunar polar lighting conditions using Clementine image data had been mainly

*Corresponding author. Tel.: +86 8515891338.
E-mail address: wangshijie@vip.skleg.cn (S. Wang).

0032-0633/$ - see front matter
doi:10.1016/j.pss.2008.02.008

made by Bussey and co-authors (Bussey et al., 1999, 2001, 2003, 2004, 2005; Fristad et al., 2004). In order to definitively understand the lunar illumination environment, more data are required. Wide area imaging coverage over an entire year is necessary to identify all regions of illumination extremes. But the data are yet not enough for the global analysis. Additionally lighting simulations using high-resolution topography could produce quantitative illumination maps.

Zuber and Smith (1997) had proposed a theoretical model based on the geometric characters of crater. They term the horizon elevation required for permanent shadow at the lunar south pole in the elevation angle, the co-latitude, and the angular distance to the crater rim. Compared with their model, the model proposed in our study is simpler and easier to compute. It is parameterized with selenographic coordinates, elevations, and time. With high-resolution topography data, the solar illumination conditions at any selenographic coordination could be estimated easily by this model at any time.

2. Primary analysis

Solar illumination on the Moon is related to the solar altitude and the lunar topography. The solar altitude is required to determine the solar illumination condition at a lunar site. It could be expressed as a function of solar incidence angle, as follows:

$$\delta = \frac{\pi}{2} - i \quad (1)$$

where δ is the solar altitude; i is the solar incidence angle for a horizontal plane on the lunar surface and could be determined by the geometric relationship in the Sun–Earth–Moon system (Fig. 1), as follows:

$$i = \alpha + \beta \quad (2)$$

where

$$\alpha = \arccos[-\sin\varphi_A \sin\varphi_d + \cos\varphi_A \cos\varphi_d \times \cos(\lambda_A - \lambda_d)] \quad (3)$$

$$\beta = \arcsin\left[\frac{R_{moon}\sin\alpha}{(R_{sm}^2 + R_{moon}^2 - 2R_{sm}R_{moon}\cos\alpha)^{1/2}}\right] \quad (4)$$

In Eqs. (3) and (4), λ_A and φ_A are the selenographic longitude and latitude at the lunar site A; R_{moon} is the mean radius of the Moon; λ_d and φ_d are the selenographic longitude and latitude at the subsolar site, respectively; R_{sm} is dimensionless distance of the Sun–Moon relative to 1 AU. The latter three parameters could be gotten by celestial mechanics. All of them are functions of time (Bretagnon and Francon, 1988; Chapront-Touzé and Chapront, 1983; Meeus, 1991). Therefore, the solar altitude is finally determined by the time, the selenographic longitude and latitude at the lunar site A. It could be simply written as $\delta(\lambda_A, \varphi_A, t)$, where t refers to the time.

The solar illumination condition of a horizontal plane on the lunar surface could be estimated from the equations above. A horizontal plane is illuminated when the solar altitude is non-zero and otherwise shadowed when the solar altitude is zero.

Once the solar altitude has been obtained, the solar illumination conditions of lunar surface could be estimated from lunar topography. The high elevations of lunar surface in solar incidence direction would shadow the lunar sites with low elevation behind them (Fig. 2). As shown in Fig. 2, the relationship between the radii of sites A and B could be written as:

$$\cos\theta = \frac{R_A}{R_B} \quad (5)$$

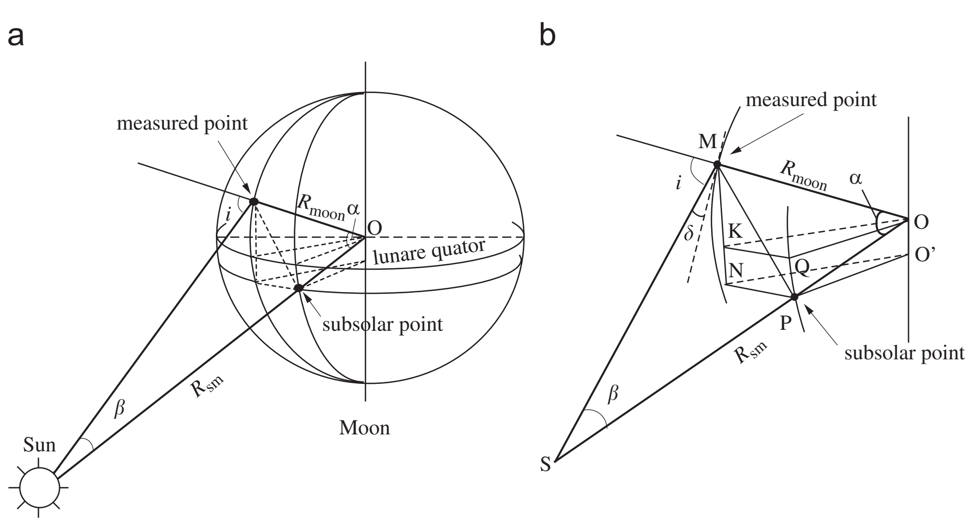

Fig. 1. Schematic diagram of solar radiation incidence angle on the lunar surface. O is the geometric center of the Moon, plane KOQ is located on the equatorial plane of the Moon, plane NO′P is parallel to the equatorial plane of the Moon, K and N are the projections of M on each plane, Q is the projection of P on the equatorial plane of the Moon, ∠KOQ and ∠NO′P are the difference between the selenographic longitudes of measured point and subsolar point, ∠MOK and ∠POQ are selenographic latitudes of measured point and subsolar point, respectively.

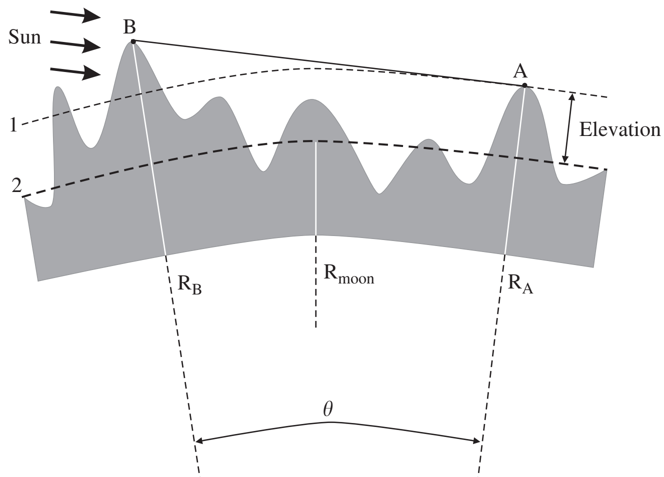

Fig. 2. Arc 1 refers to a part of great circle passed sites A and B, the sun light transfers from site B to site A; arc 2 is a part of great circle with a mean radius, line BA is a tangent to arc 1 at site A; θ refers to the angular distance between the lunar sites A and B.

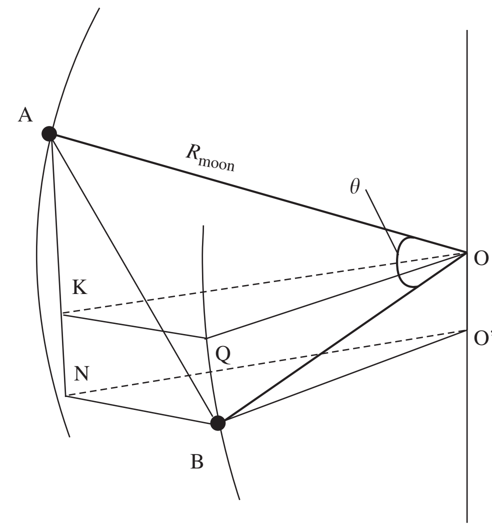

Fig. 3. O is the geometric center of the Moon, plane KOQ is located on the equatorial plane of the Moon, plane NO′B is parallel to the equatorial plane of the Moon, K and N are the projections of A on each plane, Q is the projection of B on the equatorial plane of the Moon, ∠KOQ and ∠NO′B are difference between the selenographic longitudes of lunar sites A and B, ∠AOK and ∠BOQ are selenographic latitudes of lunar site A and B, respectively.

where R_A and R_B are the lunar radii at sites A and B, respectively; θ is the angular distance between two lunar sites in solar incidence direction.

Archinal et al. (2007) have developed a unified lunar control network (ULCN2005) and lunar topographic model based on Clementine images and the previous ULCN network, which had been derived from Earth-based, Apollo photographs, Mariner 10, and Galileo images of the Moon. Their model infers that the maximum difference of radius is about 17.53 km, with the minimum lunar radius of 1724.64 km at the lowest lunar site (48.90°N, 3.83°E) and 1747.49 km for the maximum lunar radius at the highest lunar site (13.91°N, 97.68°E) related to geometric center of the Moon. So, the maximum θ is about 8°, when R_1 and R_2 are 1724.64 and 1747.49 km, respectively. The distance on the lunar surface corresponding to 8° of the θ is about 240 km estimated by tangent relationship in Fig. 2. These infer that the maximum distance between two lunar sites is about 240 km in estimation of lunar topographical shadow.

In practical application, it would be unnecessary to calculate all the topographical influence within 240 km radius. Statistical analysis of Clementine topography data shows that the maximum difference of elevation within 240 km radius is about 13323.6 m, with the low elevation of −6215.2 m at 4.125°N, 139.375°W and the high elevation of 7108.4 m at 2.125°S, 139.375°W. Considering the angular diameter of the Sun, such a difference of elevations infers about 7° of θ is enough for estimating lunar topographical shadow. In the area with $\theta < 7°$, the sites might be shadowed by the front-sites in solar irradiance direction, if elevations of front-sites are high enough. Corresponding to 7° of θ, the distance on lunar surface is about 210 km. Therefore, it is enough to take the elevations within 210 km in solar irradiance direction into account when estimating the lunar topographical shadow.

The lunar radius could be expressed as the sum of the mean lunar radius and the lunar terrain elevation. Hence, Eq. (5) could be written as follows:

$$\cos\theta = \frac{R_{moon} + H_A}{R_{moon} + H} \tag{6}$$

where H_A is the elevation at lunar site A; H is the critical elevation at the other site; θ could be determined by the selenographic longitude and latitude of lunar sites A and B (Fig. 3), as follows:

$$\cos\theta = -\sin\varphi_A \sin\varphi_B + \cos\varphi_A \cos\varphi_B \times \cos(\lambda_A - \lambda_B) \tag{7}$$

where λ_A, φ_A, λ_B, and φ_B are the selenographic longitude and latitude of lunar sites A and B, respectively.

Therefore, the following equation could be derived from Eqs. (6) and (7).

$$H = \frac{R_{moon} + H_A}{-\sin\varphi_A \sin\varphi_B + \cos\varphi_A \cos\varphi_B \cos(\lambda_A - \lambda_B)} - R_{moon} \tag{8}$$

Eq. (8) infers that H is a function of H_A, λ_A, φ_A, λ_B, and φ_B. By comparing the elevation at site B to the critical elevation, it could be estimated whether the lunar site A is shadowed by the frontal site B or not. The site A would be shadowed when the elevation at site B is higher than H, otherwise it is illuminated.

3. Model description

According to the above analysis, the solar illumination condition on the lunar surface is controlled by the solar altitude and the topographical shadow. To describe the solar illumination condition mathematically, the solar altitude factor (fs) and the topographical factor (ft) are defined as follows:

$$fs(\lambda_A, \varphi_A, t) = \begin{cases} 0, & \delta = 0 \\ 1, & \delta > 0 \end{cases} \tag{9}$$

$$ft(\lambda_A, \varphi_A, H_A, \lambda_B, \varphi_B, H_B) = \begin{cases} 0, & H_B \geqslant H \\ 1, & H_B < H \end{cases} \tag{10}$$

where δ and H are determined by Eqs. (1)–(4) and (10), respectively; H_B is the elevation at lunar site B. fs is a function of the time, the selenographic longitude and the selenographic latitude at the lunar site A. And ft is a function of the selenographic longitude, the selenographic latitude, and the elevation at the lunar sites A and B.

Finally, the solar illumination model could be simply expressed as follows:

$$F = fs(\lambda_A, \varphi_A, t) \times ft(\lambda_A, \varphi_A, H_A, \lambda_B, \varphi_B, H_B) \tag{11}$$

The solar illumination condition could be inferred by Eq. (11). It is a function of the time, the selenographic longitude, the selenographic latitude, and the elevation at the lunar sites A and B. The lunar surface is illuminated by the Sun if F is 1, and shadowed when F is zero.

4. Conclusion

Solar illumination on the Moon is controlled by the solar altitude and the lunar topography. Based on the solar altitude, solar illumination condition of lunar surface is determined by comparing the elevations within 210 km in solar irradiance direction to the critical elevations. The solar altitude and topographical factors are introduced to simply describe the solar illumination model. This model is parameterized with selenographic coordination, elevations, and time. With high-resolution topography data, the solar illumination conditions at any selenographic coordination could be estimated by our model at any time. The lunar surface is illuminated when the solar altitude is non-zero and all the elevations within 210 km in solar irradiance direction are smaller than the critical elevations. Otherwise, it is shadowed.

Acknowledgements

We thank Marria Zuber of MIT and David Paige of UCLA for helpful discussions, and the anonymous reviewers for their constructive suggestions. This work was supported by the Pilot Project of Knowledge-Innovation Program of Chinese Academy of Sciences (Grant no. KZCX2-YW-110), the National High Technology Research and Development Program of China (863 Program) (Grant no. 2007AA12A213), and the National Natural Science Foundation of China (Grant no. 40673053).

References

Archinal, B.A., Rosiek, M.R., Kirk, R.L., Hare, T.L., Redding, B.L., 2007. Final completion of the unified lunar control network 2005 and lunar topographic model. LPSC, 1904.

Arnold, J.R., 1979. Ice in the lunar polar regions. J. Geophys. Res. 84, 5659–5668.

Bretagnon, P., Francon, G., 1988. Planetary theories in rectangular and spherical variables VSOP 87 solutions. Astron. Astrophys. 202, 309–315.

Bussey, D.B.J., Spudis, P.D., 2004. The Lunar Polar Illumination Environment: What We Know & What We Don't, Space Resources Roundtable VI, 6022.

Bussey, D.B.J., Spudis, P.D., Robinson, M.S., 1999. Illumination conditions at the lunar south pole. Geophys. Res. Lett. 26 (9), 1187–1190.

Bussey, D.B.J., Robinson, M.S., Edwards, K., Cook, A.C., Watters, T., 2001. Simulation of illumination conditions at the lunar south pole. LPSC, 1907.

Bussey, D.B.J., Lucey, P.G., Steutel, D., Robinson, M.S., Spudis, P.D., Edwards, K.D., 2003. Permanent shadow in simple craters near the lunar poles. Geophys. Res. Lett. 30 (6), 1278.

Bussey, D.B.J., Robinson, M.S., Fristad, K., Spudis, P.D., 2004. Permanent sunlight at the lunar north pole. LPSC, 1387.

Bussey, D.B.J., Fristad, K.E., Schenk, P.M., Robinson, M.S., Spudis, P.D., 2005. Constant illumination at the lunar north pole. Nature 434, 842.

Butler, B.J., 1997. The migration of volatiles on the surfaces of Mercury and the Moon. J. Geophys. Res. 102, 19283–19291.

Chapront-Touzé, M., Chapront, J., 1983. The Lunar ephemeris ELP 2000. Astron. Astrophys. 124, 50–62.

Feldman, W.C., Maurice, S., Binder, A.B., et al., 1998. Fluxes of fast and epithermal neutrons from Lunar Prospector: evidence for water ice at the lunar poles. Science 281, 1496–1500.

Feldman, W.C., Lawrence, D.J., Elphic, R.C., et al., 2000. Polar hydrogen deposits on the Moon. J. Geophys. Res. 105, 4175–4195.

Feldman, W.C., Maurice, S., Lawrence, D.J., et al., 2001. Evidence for water ice near the lunar poles. J. Geophys. Res. 106, 23231–23251.

Fristad, K., Bussey, D.B.J., Robinson, M.S., Spudis, P.D., 2004. Ideal landing sites near the lunar poles. LPSC, 1582.

Hodges, R.R., 2002. Ice in the lunar polar regions revisited. J. Geophys. Res. 107, E2.

Kruijff, M., Ockels, W.J., 1995. Lunar Visibilities and Lighting Conditions. LPI, pp. 807–808.

Margot, J.L., Campbell, D.B., Jurgens, R.F., Slade, M.A., 1999. Topography of the lunar poles from radar interferometry: a survey of cold trap locations. Science 284, 1658–1660.

Meeus, J., 1991. Astronomical Algorithms. Willmann-Bell Inc., VA, USA.

Starukhina, L., 2001. Water detection on atmosphereless celestial bodies: alternative explanations of the observations. J. Geophys. Res. 106 (E7), 14701–14710.

Vasavada, A.R., Paige, D.A., Wood, S.E., 1999. Near-surface temperatures on Mercury and the Moon and the stability of polar ice deposits. Icarus 141, 179–193.

Watson, K., Murray, B.C., Brown, H., 1961. The behavior of volatiles on the lunar surface. J. Geophys. Res. 66, 3033–3045.

Zuber, M.T., Smith, D.E., 1997. Topography of the lunar south polar region: implications for the size and location of permanently shade areas. Geophys. Res. Lett. 24 (17), 2183–2186.